PREPARATION AND CHARACTERIZATION OF HEMICELLULOSE-BASED PRINTABLE FILMS

RUOXI MA, ALEXANDRA PEKAROVICOVA, PAUL DAN FLEMING III and VERONIKA HUSOVSKA

Chemical and Paper Engineering Department, Western Michigan University, 4601 Campus Drive, Parkview, Kalamazoo, MI 49008-5462, United States of America
✉ *Corresponding author: A. Pekarovicova, a.pekarovicova@wmich.edu*

Received October 5, 2016

Flexible plastic films, such as LDPE and PET, have been the most common substrates used in the printing and packaging industry for the last few decades. However, the global sustainability calls for more environmentally friendly, biodegradable and biocompatible materials. This research aims to advance the knowledge of the material properties of hemicellulose-based biofilms. Laboratory preparation of the hemicellulose-based films and the characterization of mechanical and surface properties were done. The biodegradable glucomannan films were formed with or without nanofibrillated cellulose (nanocellulose). In all cases, nanocellulose improved the mechanical properties of the films. Gravure printing was demonstrated on the biofilms. The one-way ANOVA method was used to analyze the effect of glucomannan, sorbitol as a plasticizer, and nanofibrillated cellulose on the mechanical properties of the films. It was found that all of those factors significantly affected the mechanical properties of the biofilms.

Keywords: glucomannan, nanocellulose, packaging film, surface free energy, physical properties, gravure printing

INTRODUCTION

Flexible PET (polyethylene terephthalate) or LDPE (low-density polyethylene) films are currently the main substrates for food and pharmaceutical packaging. Plastics have been the dominant packaging materials due to their much better barrier properties compared to those of traditional paper packaging. However, common plastic films cannot be easily degraded, which causes serious pollution and sustainability issues. For example, the incineration of some plastics, such as PVC, increases the dioxin and furan content of air emissions. Therefore, the global sustainability focus relies more on biodegradable and biocompatible materials. Natural polymers, such as polysaccharides, are ideal starting materials for these kinds of composites due to their biodegradability, biocompatibility, non-toxicity and renewability.[1] However, films made of pure hemicelluloses lack flexibility and have poor thermo-mechanical properties, thus they need to be modified. Xylan films alone without modification are brittle, but they can be derivatized to reach decreased water uptake, and increased flexibility. Enhanced mechanical properties of hardwood xylan films can be achieved with addition of nanofibrillated cellulose, nano-crystalline cellulose,[2-3] and sorbitol as a plasticizer,[4] or plant protein such as gluten.[5] Micro- and nanofibrillated celluloses have been successfully applied for film reinforcement in composite materials.[6] Hemicelluloses may be obtained from plant material by chemical or by more gentle enzymatic treatment,[7] or a combination of both. Obviously, the original source of xylan, or other hemicelluloses can dramatically affect the mechanical properties of the composite films.[8] Linear xylans are available from corncobs, glucuronoxylans from hardwoods, arabinoxylans from barley, oat, rye, and other cereal brans.[9-10] Depending on the particular plant material, the chemical composition of hemicelluloses vastly differs, as shown in Table 1.[11] Biodegradable films were prepared from galactoglucomannans and xylans isolated from wheat straw and blended with carrageenan and locust bean gum.[12] The film-forming properties of xylan hemicelluloses can be enhanced by acetylation,[13] or by reinforcing with cellulose nanofibrils. Galactoglucomannans were hydrophobized and used for packaging applications as well.[14]

Table 1
Hemicelluloses and their sources[11]

Type of hemicellulose	Source	Amount (%)
Arabinoglucuronoxylan	Softwood	7-10
Arabinogalactan	Larchwood	5-35
Arabinoxylans	Annual plants, bran	Variable
Galactoglucomannan	Softwoods	20
Glucomannan	Hardwood	2-5
Glucuronoxylan	Hardwoods	15-30

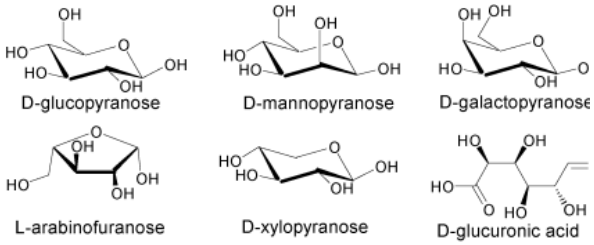

Figure 1: Main components of hemicelluloses[17]

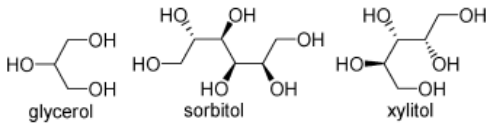

Figure 2: Commonly used plasticizers for hemicellulose-based films[18]

Lignocellulosic biomass from trees, annual grasses, cereals, and other plants has become the main focus of the developing bio-refining industry.[15] As the main components of plants, cellulose, lignin and hemicelluloses have received a lot of attention in terms of material applications. Hemicellulose is defined as the alkali-soluble polysaccharide remaining after the elimination of pectic substances from plant cell walls.[16] Hemicelluloses (Fig. 1), depending on their plant material source and sugar composition, can be divided into five main groups, which can be defined according to their primary structure as follows: arabinoglucuronoxylans, galactoglucomannans, arabinogalactans, glucomannans and glucuronoxylans.[17-18]

The research on hemicelluloses and their packaging and medical applications has been extensive. The konjac glucomannan, which is derived from the plant of genus Amorphophallus, has been used commercially for many years owing to its gel- and film-forming properties, as well as biocompatibility and biodegradability.[17] There are several ways to obtain hemicelluloses from plant resources, including extraction with alkali, dimethyl sulfoxide or methanol/water, as well as steam or microwave treatment.[19] Depending on different pretreatment procedures, the composition of the hemicelluloses could be varying. Sun *et al*. reported the dependency of composition on the isolation procedure, as the pretreatment of wheat straw samples with various organic solvents before extraction resulted in very different hemicellulosic products.[20]

Hemicelluloses are hydrophilic in nature, hence hemicellulose-based films are generally hygroscopic, which means they will absorb moisture and degrade with high humidity. This is because they have abundant free hydroxyl groups distributed along the main and side chains and they are ideal candidates for chemical functionalization. Many researchers have been focusing on modifying the properties such as crystallinity, solubility and hydrophilicity of hemicelluloses through techniques such as esterification, etherification or grafting. Through chemical modifications, the hemicellulose-based films could have lower oxygen permeability, lower water vapor permeability and higher mechanical strength and flexibility. Grondahl *et al*. reported films made of glucuronoxylan from aspen wood, showing improved oxygen barrier properties and the addition of plasticizer resulted in increased tensile strength.[21]

Hemicelluloses, besides cellulose and lignin, are the main components of the plant cell wall, and are bound to lignin. The composition of hemicelluloses is different in various raw materials. For example, a study by Lai *et al*. reported that the main components vary a lot in four kinds of rice straw, containing arabinose (5-23%), xylose (17-40%), and glucose (36-55%).[22]

Films made on the basis of hemicellulose with addition of plasticizers were reported as early as 1949 by Smart and Whistler.[23] The reason to use plasticizers in hemicellulose-based films is to ensure flexibility and the most commonly used plasticizers are sorbitol, glycerol and xylitol (Fig. 2). Besides packaging applications,[18,24] biodegradable hemicellulose films can be used for biomedical applications

due to their non-toxicity, biodegradability and biocompatibility.[25] Biomedical applications include controlled drug release, or improved medical imaging.[26]

In this work, biodegradable glucomannan films were formulated with and without nanofibrillated cellulose, with the aim to reinforce the mechanical strength of the film and impart improved barrier properties to the film. Another aim was to characterize selected physical properties of the formulated films and assess possible printability.

EXPERIMENTAL

Biofilm preparation

Glucomannan was prepared from a solution (0.5-1% w/w) from NOW Foods, Inc. (Fig. 3) in a 250 ml beaker during continuous stirring at 25 °C.[23] Nanofibrillated cellulose (NFC) manufactured by the Department of Chemical and Biological Engineering, University of Maine (containing water 95-99% and cellulose pulp 1-5%), in suspension form, was added to the glucomannan separately. Then, 1% lignin in powder form with 95% purity (Sigma Aldrich) and 0.1% Surfynol® CT111 (Air Products and Chemical, Inc.) were added. The formulations of the films (Table 2) were designed with different dosage of NFC, glucomannan and plasticizers, with the objective of observing how they affect strength properties. The mixture was further homogenized using a magnetic stirrer (Corning Model PC-420) at 45 °C and a mixing speed of 600 RPM. The solutions were cast on a mold with the dimensions of 100 mm × 100 mm. Films were dried in Environmental Test Chambers (Caron Model 6010), for 8 hours at 60 °C and 35% RH. Dried hemicellulose-based films were peeled off manually and stored in polyethylene bags prior to characterization.

Films characterization

Selected mechanical properties and surface energy of the films were tested. A PET film (from Dupont LLC) and uncoated paper with a basis weight of 118 g/m^2 (from Western Michigan University Pilot Plant) were also analyzed as control samples. For each test, five replicates were done per each film.

Surface free energy

When it comes to printing, it is essential to understand the behavior of ink on the chosen substrate. Surface energy/tension is responsible for the surface behavior (atmosphere-solid contact) and the wetting phenomena (liquid-solid contact), as illustrated in Figure 10.[28]

The surface energy of the films was estimated by a FTA200 (First Ten Angstrom Dynamic Contact Angle) measurement apparatus. Pendant drop analysis was used for the surface tension measurements of liquid phases. Sessile drop analysis was used for the contact angle measurements. The actions of the droplet appear live on the computer screen and salient images are captured to the computer's memory for later image analysis. The camera frame rate is 60.9 frames per second.

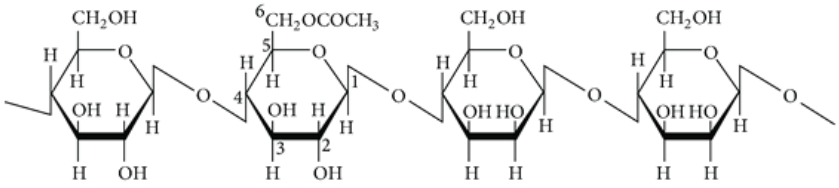

Figure 3: Glucomannan composed of β-D-glucopyranose and β-D-mannopyranose units linked by 1→4 β-D-glycosidic bonds (second glucopyranose unit is esterified)[23]

Table 2
Formulation of biofilms

Ingredient (g)	Film 1	Film 2	Film 3	Film 4
Water	100	100	100	100
Xylan	1	1	0	0
Sorbitol	0.5	0.5	0	1
Glucomannan	0.5	1	0.5	1
Lignin	1	0	0.5	1
Nanocellulose	0	0.1	0	0.2
Surfactant	0.1	0.1	0.1	0.1

The surface energy is calculated by the program by the Owens-Wendt method, using 1 angle of each of 2 liquids on 1 solid. For each kind of liquid, the software captured 300 images of the fluid dropping, hitting the substrate and reaching equilibrium on the substrate. The measurement was conducted under conditions of 23 °C and 25% RH.

The FTA200 is a flexible video system for measuring contact angle, surface and interfacial tensions, wettability and absorption. For the evaluation of the surface energy, the contact angle of three liquids, deionized ultra-filtered water (DI), hexadecane and methylene iodide (MI), was measured against the biofilm surfaces, and the critical surface free energy was calculated using the Owens-Wendt method.[27] Although these methods only estimate the solid surface energy, such values are useful for comparing the wettability of solid surfaces and predicting print adhesion.

Contact angle measurement is the ideal method for the characterization of surface energy and surface wettability, and is a widely used technique for studying the loss and recovery of hydrophobicity of the films. Therefore, this method can be used to accurately measure the hydrophilic characteristic of a surface of a hemicellulose-based film. This method enables the surface energetics of a solid surface to be determined by its free surface energy. Often, it is defined on the basis of the static contact angle between the surface and a liquid droplet. The fundamental equation for measurement of solid surface tension by contact angle measurements is described by Young's equation.[28] Contact angles of deionized ultra-filtered water (DI), hexadecane and methylene iodide (MI) were measured against the biofilm surfaces, and the critical surface energy was calculated using Owens-Wendt method measurements on a solid substrate (Table 5).[27]

Tensile strength

The tensile strength and elongation at break of the films were assessed according to TAPPI Standard T494 at 25 °C and 50% RH, using an INSTRON 430I with a 500 N load cell. The specimens were conditioned under 25 °C and 50% RH for 24 hours prior to testing. The initial gauge length was 100 mm, and the crosshead speed was 25 mm/min. The width of each specimen was 15 mm.

Bursting strength

The bursting strength of the biofilms was measured using the Mullen Tester according to TAPPI Standard T403.

Gravure printing

Gravure printing was demonstrated with a laboratory gravure proofing press K-Printing Proofer (Testing Machines Inc.) at a speed of 40 m/min. The image on the plate is a solid patch with a fine resolution of 200 lines per inch. Black gravure ink was acquired from Western Michigan University Pilot Plant. The ink is toluene based with a viscosity of 15 centipoise. The printed films were placed in the laboratory under controlled conditions (23 °C, 50% RH) for 24 hours conditioning prior to optical density measurement with an X-Rite 530 SpectroDensiometer. The density measurement conditions were the following: absolute mode, with statue T and with a white backing.

RESULTS AND DISCUSSION

Four different hemicellulose formulations (Table 2) were designed with different dosage of NFC, glucomannan and plasticizer, with the aim to investigate their effect on the strength properties of the resulting films and evaluate the printability of the latter. Films were formulated with various amounts of xylan, glucomannan, nanocellulose, lignin, sorbitol and surfactant. It was observed that the xylan and lignin made the films more brittle, and, on the other hand, nanocellulose showed a strengthening effect on the films. To find out if individual components were statistically important and how they affected the strength of the films, ANOVA analysis was performed.

Optimization of biofilm formulation

The main factors in the film formulations are the portion of nanocellulose, sorbitol and glucomannan. In order to analyze the results of the film formulation, one-way ANOVA analysis of tensile strength *versus* the main factors was performed using the Minitab® 17 software package (Minitab Inc.). The full ANOVA was not performed because there were no degrees of freedom for the factors. ANOVA analyses were performed on the data pertaining to nanocellulose content *versus* tensile strength, amount of sorbitol as a plasticizer, and level of glucomannan added (Table 3). The significance level for each ANOVA was set as 0.05. The results are shown in Table 4. Although the preliminary formulations of the biofilm represent an unbalanced design, it is instructive to investigate which factors contributed to the tensile strength and thus optimize the film formulation design in the

future work. For nanocellulose and sorbitol, there are 3 levels of the factor and 5 replicates for each level. For glucomannan, there are 2 levels and 5 replicates for each level (Table 3). The program computed the F ratio. F-Value equals 176.88 and we can compare this result to an appropriate upper-tail percentage point of the $F_{2,12}$ distribution. Suppose $\alpha = 0.05$, $F_{0.05,2,12} = 3.89$.[29] Because $F_0 = 176.88 > 3.89$, we reject H_0 and conclude that the treatment means differ, that is, the amount of nanocellulose significantly affects the mean tensile strength of the films. For the tensile strength *versus* sorbitol, $F_0 = 216.62 > F_{0.05,2,12} = 3.89$, which means the amount of sorbitol also significantly affects the mean tensile strength of the films (Table 5). For the tensile strength *versus* glucomannan, $F_0 = 165.5 > F_{0.05,1,8} = 5.32$, which means the amount of glucomannan significantly affects the mean tensile strength of the films as well (Table 6).[29]

Tensile strength

Tensile tests measure the force required to break the sample specimen and the extent to which the specimen stretches or elongates to that breaking point. The tensile strength data can help specify optimal film formulations. Tensile strength values of the films are shown in Figure 4. Compared to xylan and lignin, nanocellulose has a clearly better strengthening effect on the films. The tensile strength of the hemicellulose films is much lower than that of the PET film, but it is relatively comparable with that of the kraft paper. Among the four hemicellulose film formulations, film #4 had the highest tensile strength, probably due to the highest addition of nanofibrillated cellulose. Film #1 made with lignin and sorbitol lacked flexibility. Film #3 made with glucomannan and lignin without plasticizer was brittle.

Table 3
Factors and levels in ANOVA analysis for the film formulations

Factor	Level (mass fraction %)		
Nanocellulose	0	0.1	0.2
Sorbitol	0	0.5	1
Glucomannan	0.5	1	N/A

Table 4
ANOVA results for tensile strength *versus* nanocellulose

Source	Degree of freedom	Adj. SS	Adj. MS	F-value	P-value
Nanocellulose	2	0.00644	0.00322	176.88	0.000
Error	12	0.00022	0.00002		
Total	14	0.00666			

Table 5
ANOVA results for tensile strength *versus* sorbitol

Source	Degree of freedom	Adj. SS	Adj. MS	F-value	P-value
Sorbitol	2	0.01264	0.00632	216.62	0.000
Error	12	0.00035	0.00003		
Total	14	0.01299			

Table 6
ANOVA results for tensile strength *versus* glucomannan

Source	Degree of freedom	Adj. SS	Adj. MS	F-value	P-value
Glucomannan	2	0.00388	0.00388	165.50	0.000
Error	12	0.00019	0.00002		
Total	14	0.00407			

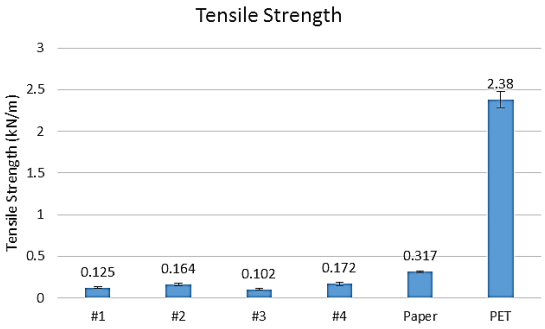

Figure 4: Tensile strength of the hemicellulose based films, paper and PET film

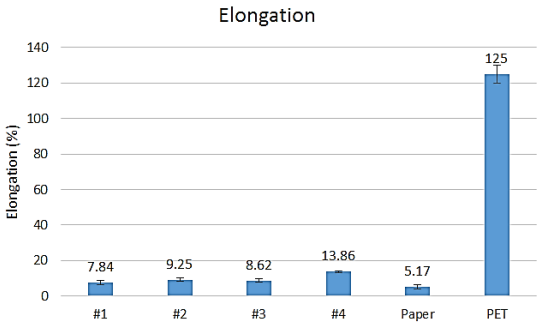

Figure 5: Elongation of the hemicellulose-based films, paper and PET

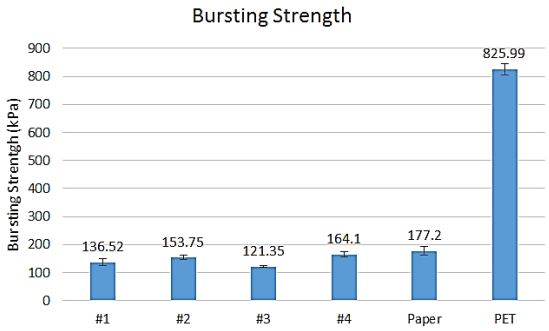

Figure 6: Bursting strength of the hemicellulose-based films, paper, and PET film

Elongation

Elongation is the ratio between changed length and initial length after breakage of the test material. It expresses the capability of a material to resist the changes of shape without crack formation. For elastomers and packaging films (*e.g.* LDPE), the ultimate elongation values could be several hundred percent. For rigid plastic, such as fiber reinforced PET films, the elongation values are under 5%. The combination of high tensile strength and high elongation leads to materials with high toughness. The elongation of the hemicellulose biofilms was higher than that of paper (Fig. 5), but much lower than that of the PET film. The highest elongation was found for film formulation #4 with the highest amount of nanofibrillated cellulose.

Bursting strength

The bursting strength is defined as the hydrostatic pressure needed to burst a sample when it is applied uniformly across its side. The bursting strength is measured by using a rubber diaphragm that is expanded hydraulically against the sample. Bursting strength tests are generally used for paper and board where there are definite warp and weft directions due to fiber bonding. Hoverer, the biofilms were cast onto aluminum foil covered mold. It was like a handmade sheet in the laboratory without obvious orientation. In other words, the film is homogeneous, which means, during the bursting test, the film undergoes the same extension in all directions. This could be proven by the uniform rupture of the film samples. The bursting strength of the biofilms was close to that of the kraft paper, which could be evidence for the statement that those films could function as packaging materials. Among all the formulations, film #4 has the highest bursting strength, which is coherent with its highest tensile strength. However, there is still a long way to go for all the biofilms to be comparable with the PET film (Fig. 6).

Air permeability

Permeability describes how easily a fluid is able to move through the porous material. It is calculated using a formula widely known as Darcy's Law:

$$Q = K\Delta P^{*}A/\eta\Delta L \qquad (1)$$

where Q = flow rate (m^3/s); K = permeability coefficient, (m^2); ΔP = pressure drop or difference, (Pa); L = flow length or thickness of test sample, (m); A = area of cross-sectional area to flow, (m^2); η = fluid viscosity, (Pa-s).

The standard parameters used for the PPS tester were as follows:[30] fluid (air) viscosity (η) of 1.80075 E-05 Pa-s (Ns/m^2) at 23 °C, standard pressure drop (ΔP) of 6.17 kPa, and area of cross-section (A)of 10 cm^2.

Therefore, the permeability coefficient[31] could be calculated:

$$K\ (\mu m^2) = 0.048838 * Q\ (ml/min) * L\ (m)^1 \qquad (2)$$

An example calculation of the permeability coefficient for a hemicellulose-based film using Equation (2) follows:

Parker Print Surf flow rate (*Q*) at 1000 kPa: 0.59 ml/min

Thickness of the sample film (*L*): 223.6 µm

Permeability coefficient $K = 6.44 \times 10^{-06}$ μm^2

Air permeability is a good measure of how much and how quickly inks are absorbed into a substrate. However, plastic films are considered non-porous substrates because of their low porosity in terms of both air and liquid penetration.

This non-porous property enables the films to function as packaging substrate for special products, such as foods, pharmaceutical products and chemicals. All the films are non-porous (Fig. 7), which means that they have potential to serve as food packaging with good barrier property.

Roughness

For contacting-type printing processes, such as offset lithography or gravure printing, the ink film will transfer to the substrate surface upon physical contact. When the voids in the substrate surface are deep enough to prevent such contact, the ink transfer will not be uniform and will cause poor print quality. The roughness (Ra) of the biofilm was measured using a Messmer Parker Print-Surf (PPS) with soft backing and 1000 kPa clamping pressure. Compared to film #1, the surface of films #3 and #4 is less even (Fig. 8). This is because of the bubbles that were introduced into the suspension during the mixing and drying stages of the film forming process. The wire side is smoother than the top side due to its contact with the supporting foil backing. Meanwhile, the top side has many tiny bubbles that were introduced into the suspension during the mixing and spreading process, which leads to a rougher surface on the top side and makes it more difficult to print on.

Caliper

The caliper of the biofilms was measured by a Technidyne PROFILE/Plus Thickness instrument. The caliper of the films was controlled during film formation using a Meyer rod, in this case, Meyer rod #6, as well as with the solids content of the suspension. The films with NFC (#2 and #4) had a higher amount of glucomannan than films #1 and #3 (Fig. 9), but a lower caliper than the films without NFC (#1 and #2). It appears that NFC is responsible for better conformation and bonding of biofilms. The thickness of the films slightly increased with the amount of added NFC (films #2 and #4).

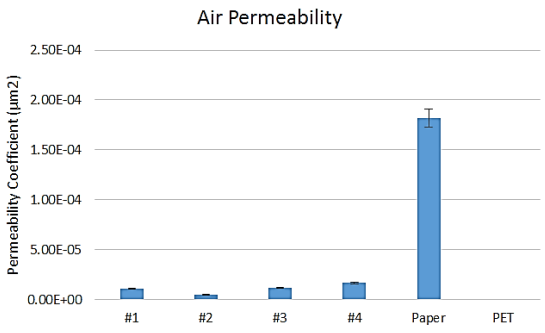

Figure 7: Air permeability of hemicellulose-based films, kraft paper and PET film

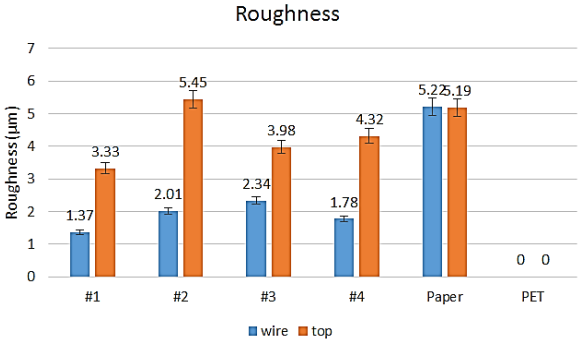

Figure 8: Roughness of hemicellulose-based films, kraft paper and PET film

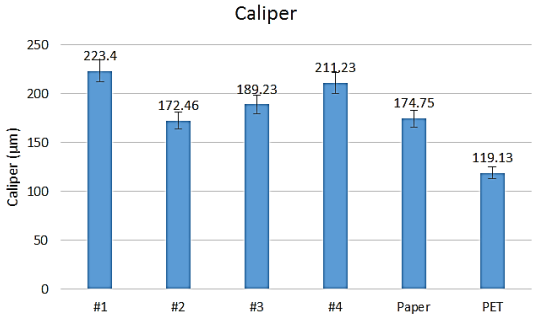

Figure 9: Caliper of hemicellulose-based films, kraft paper and PET film

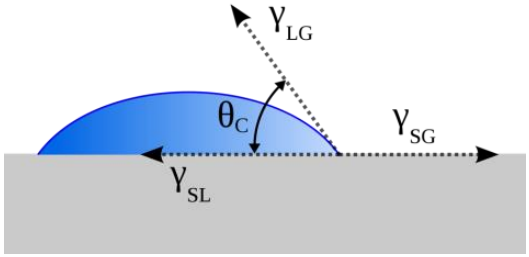

Figure 10: Contact angle of liquid on a substrate[28]

Table 7
Surface tension of liquid phases with values of dispersion and polar components used in Owens-Wendt calculations

Liquids	γ_{LV}	$\gamma_{LV\text{-}Disp.}$	γ_{LV_Polar}	Density (g/cc)
DI water (DI)	71.40±0.8	21.80	49.60	1.000
Diiodomethane (MI)	48.00±0.6	45.75	2.25	3.325
Hexadecane (HE)	21.30±0.2	21.30	0	0.770

Table 8
Owens-Wendt method of estimating surface free energy values of hemicellulose film #4

Owens-Wendt	Total (mJ/m^2)	Dispersive (mJ/m^2)	Polar (mJ/m^2)
DI/MI	55.33	32.49	22.83
MI/Hexadecane	51.49	21.10	30.39

DI – distilled water, MI – methylene iodide

Table 9
Owens-Wendt method of estimating surface energy values of PET film

Owens-Wendt	Total (mJ/m^2)	Dispersive (mJ/m^2)	Polar (mJ/m^2)
DI/MI	45.80	38.70	7.10

DI – distilled water, MI – methylene iodide

Table 10
Owens-Wendt method of estimating surface energy values of kraft paper

Owens-Wendt	Total (mJ/m^2)	Dispersive (mJ/m^2)	Polar (mJ/m^2)
DI/Methylene iodide	60.88	1.76	59.12

Surface free energy

Table 7 shows the surface tension of the liquid phases. Table 8 shows the contact angles on the biofilm substrate measured with the liquid phases. The surface tension values in Table 7 and the contact angle values in Table 8 were introduced into the FTA32 software, in which the Owens-Wendt method requires the contact angle of each of the two known liquids on the substrate to estimate the surface energy. The surface energy results of each liquid pair – MI/DI and DI/HE – were calculated by the software and presented in Table 9. The Owens-Wendt equation resulted in slightly different surface energy values for the same substrate when the probe liquids were paired differently.

Because the mechanical tests (tensile, bursting) showed that film formulation #4 produced the strongest film, this film was selected to perform the surface energy test, along with the PET and paper for comparison purposes (Table 9 and Table 10). The estimated surface free energy value of 55.33 mJ/m^2 is relatively high, which predicts excellent wetting with ink and high ink adhesion.

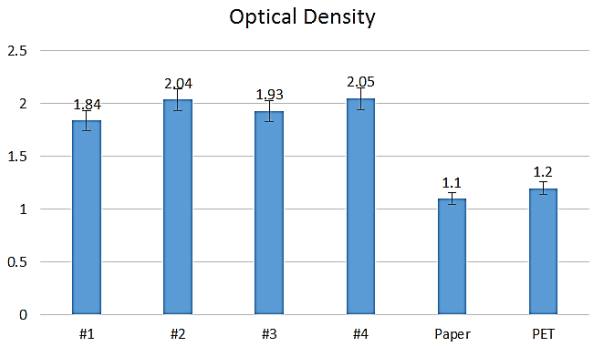

Figure 11: Optical density of solid black patch printed on glucomannan films, paper and PET

Hemicellulose is hydrophilic in nature, hence hemicellulose-based films are generally hygroscopic, which means they will absorb moisture. The water drops spread on the films and totally wet the surface. However, the methylene iodide drops bead up on the film surface. This is because the hemicellulose has abundant free hydroxyl groups distributed along the main and side chains and is affinitive to water.

Gravure printing

Preliminary printing experiments were done using a K-Printing Proofer in gravure mode, mimicking rotogravure printing. The optical density of the printed films is illustrated in Figure 11. With similar surface free energy to the paper, the biofilm has higher print density with the same gravure ink. This is probably due to the lower roughness of the film surface. Further study will investigate the topography of the biofilm surface using a Bruker white light interferometer.

CONCLUSION

Biodegradable glucomannan films were formulated with and without reinforcement with nanofibrillated cellulose. Statistical analysis of individual components addition showed that glucomannan, sorbitol and nanocellulose all significantly affected the mechanical properties of the films measured as tensile strength. Nanofibrillated cellulose increased the mechanical strength of the glucomannan films, which was attested by the increased tensile and bursting strength. The glucomannan films were non-porous, which may be a useful property for potential application as food packaging material with good integrity. The surface energy of the hemicellulose films was found to be relatively high, because the hemicellulose is hydrophilic in nature. The high surface energy of the films was beneficial for ink adhesion. The films were gravure printed with solvent based ink using a gravure K-proofing press. Print density values of the hemicellulose films were slightly lower than those found for kraft paper and PET film, but the biofilms exhibited potential to be used as packaging material.

REFERENCES

1 A. S. Juho and K. Aleksi, *Food Chem*., **151**, 343 (2014).
2 S. Vuoti, R. Talija, L. S. Johansson, H. Heikkinen and T. Tammelin, *Cellulose*, **20**, 2379 (2013).
3 J. S. Stevanic, E. M. Bergstrom, P. Gatenholm, L. Berglund and L. Salmen, *J. Mater. Sci*., **47**, 6724 (2012).
4 A. Saxena, T. Elder and A. J. Ragauskas, *Carbohyd. Polym*., **84**, 1371 (2011).
5 B. S. Kayserilioglu, U. Bakir, L. Yilmaz and N. Akkas, *Bioresour. Technol*., **87**, 239 (2003).
6 A. Khalil, A. H. Bhat and I. Yusra, *Carbohyd. Polym*., **87**, 963 (2012).
7 P. Oinonen, D. Areskogh and G. Henriksson, in *Procs. 16th International Symposium on Wood, Fiber and Pulping Chemistry*, ISWFPC, 2011, pp. 1028-1031.
8 I. Egues, A. Eceiza and J. Labidi, *Ind. Crop. Prod*., **47**, 331 (2013).
9 Z. X. Lu, K. Walker, J. Muir, T. Mascara and K. O'Dea, *Am. J. Clin. Nutr*., **71**, 1123 (2000).
10 J. Pekarovic, M. Busso, L. Raycraft and A. Pekarovicova, in *Procs. 3rd International Scientific Conference*, Slovakia, 2012, pp. 108.
11 E. Sjostrom, "Wood Chemistry", San Diego, Academic Press, 2nd ed., 1993, pp. 293.
12 H. Ruiz, H. D. Cerqueira, H. D. Silva, M. Rosa and M. Rodriguez-Jasso, *Carbohyd. Polym*., **92**, 2154 (2013).
13 A. Blazej and M. Kosik, "Fytomasa ako chemicka surovina", Veda, Slovak Academy of Science, Bratislava,

1985, pp. 402.
[14] T. Saito, R. Kuramae, J. Wohlert, L. Berglund and A. Isogai, *Biomacromolecules*, **14**, 248 (2013).
[15] A. J. Ragauskas, C. K. Williams, B. H. Davison, G. Britovsek, J. Cairney *et al*., *Science*, **311**, 484 (2006).
[16] R. C. Sun, X. F. Sun and J. Tomkinson, in "Hemicellulose: Science and Technology", edited by P. Gatenholm and M. Tenkanen, ACS Symposium Series, Washington, DC, 2004, pp. 2-22.
[17] A. Ebringerova, *Macromol. Symp.,* **232**, 1 (2006).
[18] A. Ebringerova, Z. Hromadkova and T. Heinze, *Adv. Polym. Sci.*, **186**, 1 (2005).
[19] M. S. Lindblad and A. C. Albertsson, in "Polysaccharides: Structural Diversity and Functional Versatility", edited by S. Dimitriu, Marcel Dekker, New York, 2005, pp. 491-508.
[20] X. F. Sun, F. Xu, H. Zhao, R. C. Sun, P. Fowler *et al*., *Carbohyd*. Res., **66**, 97 (2005).
[21] M. Grondahl, L. Eriksson and P. Gatenholm, *Biomacromolecules*, **5**, 1528 (2004).
[22] V. M. F. Lai, S. Lu, W. H. He and H. H. Chen, *Food Chem*., **101**, 1205 (2006).
[23] C. L. Smart and R. L. Whistler, *Science*, **110**, 713 (1949).
[24] N. M. Hansen and D. Plackett, *Biomacromolecules*, **9**, 1493 (2008).
[25] E. Ten and W. Vermerris, *Polymers*, **5**, 600 (2013).
[26] S. Arola, J. M. Malho, P. Laaksonen, M. Lille and M. B. Linder, *Soft Matter*, **9**, 1319 (2013).
[27] D. K. Owens and R. C. Wendt, *J. Appl. Polym. Sci*., **13**, 1741 (1969).
[28] T. Young, *Philos. Trans. R. Soc*., **95**, 65 (1805).
[29] D. C. Montgomery, in "Design and Analysis of Experiment", John Wiley & Sons, Inc., 2005, pp. 203-254.
[30] Operating and Maintenance Instructions for the Parker Print-Surf Roughness and Porosity Tester, H. E. Messmer Ltd., Britain, 2005.
[31] L. Pal, M. K. Joyce and P. D. Fleming, *Tappi J*., **5**, 10 (2006).